Evaluation of numerical uncertainties on the modeling of dry masonry structures submitted to out-of-plane loading, using the NSCD method in comparison with experimental test

Paul Taforel, Frédéric Dubois, Stéphane Pagano

European Congress on Computational Methods
in Applied Sciences and Engineering (ECCOMAS 2012)
J. Eberhardsteiner et.al. (eds.)
Vienna, Austria, September 10-14, 2012

EVALUATION OF NUMERICAL UNCERTAINTIES ON THE MODELING OF DRY MASONRY STRUCTURES SUBMITTED TO OUT-OF-PLANE LOADING, USING THE NSCD METHOD IN COMPARISON WITH EXPERIMENTAL TEST

P. Taforel[1,2], F. Dubois[1], and S. Pagano[1]

[1] Laboratoire de Mécanique et Génie Civil (LMGC), Université Montpellier 2, CNRS
CC 048 Place Eugène Bataillon, 34095 Montpellier Cedex 05, France.
{paul.taforel, frederic.dubois, stephane.pagano}@univ-montp2.fr

[2] GEOTER International
Espace 890, RN 96, 13360 Roquevaire, France.
paul.taforel@geoter.fr

Keywords: 3D masonry structures, Signorini-Coulomb condition, Discrete Element Method (DEM), Non-Smooth Contacts Dynamic (NSCD), LMGC90, numerical analysis

Abstract. *Masonry structures are one of the most common housing type built all around the world. Nonetheless computational methodologies implemented in classical engineering software seem not to be adapted to fine analysis of masonry structures.*

The Non-Smooth Contact Dynamics method developed by JJ Moreau and M Jean (the Discrete Element Method implemented in the software LMGC90) can perform the modeling of divided media and thus seem particularly well adapted to this type of computation.

This work aims to better understand the behavior of the algorithm used in the LMGC90 software in the resolution of this kind of problems. The impact on the local and global behaviors of structures are considered and discussed. Both the notion of reliability of model and the notion of quality of the simulation are focused on.

This work is particularly based on the comparison between experimental and numerical results obtained with the LMGC90 software. The test consists in the modeling of a simple dry masonry structure placed on a tilting table. Three interaction laws are used to model the Signorini-Coulomb condition. The stability of the wall modeled with rigid bodies is studied regarding with the influence of numerical parameters calibrating the Gauss-Seidel algorithm used to resolve such a multi-contact problem. Local behaviors are also considered as well as CPU effectiveness.

1 INTRODUCTION

Masonry structures, as a widespread construction type, cover various type of structures from the most complex civil engineering ones inherit from the past – roman aqueducts, stone bridges, ... – to more common building constructions. This very last category is usually split into specific heritage buildings and more basic housing constructions. Their proportion in the whole building stock can be explained throughout many reasons amongst historical, economical and technical ones. Even if a large part of those structures is inherit from the past, this method of house building is nowadays still one of the most usual type of construction since it appears as affordable and simple to go through with.

Due to the longevity of these buildings, they present various type of degradation (corrosion due to the action of the weather, pollution, …) and are subjected to very different loading actions (settlement, action of the wind, …) throughout the most aggressive ones such as seismic solicitations. All those mechanisms have to be better understood so that the rehabilitation of the oldest masonry structures would be efficient, and the design of the newest ones would be accurate regarding all those factors. The better understanding of the behavior of masonry structures within their specific local context and their own mechanical and physical properties is one of the main issue which has to be dealt with by civil engineers and which has to be focused on regarding their numerical modeling with relevant software.

Masonry structures as any buildings are subjected to standard construction rules which aim to insure their compliance with the best standard practices (EUROCODE 6). From the last four decades, computational methodologies have been developed and implemented in a lot of engineering software so as to help to well design structures and to understand their behavior. While those tools give relevant results for the most newly methodologies used in civil engineering (steel frame buildings, reinforced concrete buildings), they do not seem to be well adapted to masonry structures. This can be easily explained regarding the specificity of those structures built as an arrangement of heterogeneous blocks joint together in a cement-matrix.

Among all the methods developed to take into account specificities of masonry buildings, Discrete Elements Methods (DEM), as NSCD (“Non Smooth Contact Dynamics”) developed by J.J. Moreau and M. Jean, method seem to be particularly well adapted. It can perform the modeling of very large collection of bodies in interaction, with various modeling options. Each body of the collection is defined throughout a unique geometrical description and a specific bulk model (rigid/deformable) – which can differ from a body to another – whereas interaction laws (modeling friction, cohesion, etc) characterize body-body behavior. Due to this fine modeling of the structure we expect a reliable description of the masonry behavior.

Considering the structure as a multi-contact system makes possible to compute the motion of each body belonging to the collection taking into account both their own loads and their interactions with other bodies in the collection. The main effort of the method finally consists in the resolution of the underlying multi-contact problem. As usual, the quality of the whole behavior of the collection depends on the way the algorithm is operating.

This work aims to evaluate the uncertainties due to physical and numerical parameters on the modeling of specific masonry structures – dry masonry structures submitted to out-of-plane loading – , using the NSCD method implemented in the LMGC90 software. The very first purpose of this study is to illustrate the behavior of the NLGS (“Non Linear Gauss Seidel”) contact solver focusing on both the influence of algorithm calibration and on physical model choice. The influence on the local behavior (at the scale of interaction) and on the global one (at the scale of the structure) are considered. Local phenomena observed due to the use of the NLGS algorithm are illustrated on a simple study case modeling the overturning of a column. Then, comparison of numerical results with experimental ones (performed by the

University of Pavia) on 1:5 scale dry masonry structures are performed so as to study parameters influence at the scale of the structure. The experimental test consists in determining the angle for which a simple dry masonry structure placed on an inclination table machine becomes unstable. Bricks unit are modeled as rigid bodies whereas three contact laws, modeling the Signorini-Coulomb condition, are compared regarding: their influence on the NLGS algorithm, their CPU time effectiveness in the modeling and their effect on the local and global behaviors of the sample.

2 THE NON-SMOOTH CONTACT DYNAMICS

Discrete element methods constitute an interesting tool for the study of divided materials or structures as granular matter or masonry [1, 2]. Basically DEM model a material or a structure at element scale and are able to describe various behaviors (equilibrium, flow, localization of deformations, fracture, dissipation, *etc*) which can not be properly represented by a unique continuum approach even with advanced constitutive model based on a huge number of parameters.

Various numerical strategies are available to deal with the dynamics of such collections of solids. Deriving a relevant numerical model raises many issues especially due to the fact that it mixes various time and space scales. In the present work we focus on a fully implicit method, the NSCD approach, initiated by J.J. Moreau and M. Jean [3, 4, 5, 6], and implemented in the LMGC90 software [7, 8, 9]. The interaction laws are written as multi-valued functions relating the local unknowns (impulse over the time step and the relative velocity), in the framework of Non-Smooth Dynamics proposed by J.J. Moreau. These impulses account for all events supposed to occur during a time step, free flight, single or numerous impacts between pairs or agglomerates of contacting bodies. The method allows reasonably large time steps.

The resolution of the multi-contact problem consists indeed in solving two sets of unknowns – global ones (or kinematic space unknowns) related to the bodies and local ones (or contact space unknowns) related to interactions – linked together thanks to kinematic and duality relationships (H and ${}^{T}H$ operators, Figure 1, [10]).

$$H(q): \ \{R\alpha\} \rightarrow r = \sum_{\alpha} H^{\alpha}(q)\, R^{\alpha}$$

$${}^{T}H(q): \ u \rightarrow \{U^{\alpha}\} = \{{}^{T}H^{\alpha}(q)\, u\}$$

$$\begin{array}{ccccc} & & q, u \leftarrow \textit{Equations of motion} & \rightarrow & r \\ {}^{T}H(q) & \downarrow & & & \uparrow \ H(q) \\ & U^{\alpha} & \leftarrow \quad \textit{Contacts laws} & \rightarrow & R^{\alpha} \end{array}$$

Figure 1: Local-Global mapping

The motion of each body of the collection of bodies in presence of contacts and with collisions and other non smooth phenomena is given – using the formalism proposed by J.J. Moreau in the NSCD method – by the following discretized in space and time equation:

$$u_{i+1} = u_{free} + \boldsymbol{M}^{-1} r_{i+1} \tag{1}$$

where u_{i+1} is the velocity of the body at the end of the time step, u_{free} is the velocity free of contact and $\boldsymbol{M}$ is an inertia like matrix, whose expression depends on the choice of modeling of the body. For rigid bodies $\boldsymbol{M} = M$ whereas for deformable ones $\boldsymbol{M} = M + h\theta C + h^2\theta^2 K$,

where M, C and K are respectively the mass, the viscosity and the stiffness matrix. r_{i+1} is an impulse resulting of all the contact impulses applied on the object over the time interval.

The resolution of the contact problem is done expressing dynamics in term of interaction unknown and using a Non-Linear Gauss-Seidel method. Afterward the solution at the body scale is computed. Dynamics in term of local unknowns is obtained using H and ${}^{T}H$ mappings:

$$U_{i+1}{}^{\alpha} = U_{free}{}^{\alpha} + \sum \boldsymbol{W}^{\alpha\beta}(q)\ R_{i+1}{}^{\beta} \qquad (2)$$
$$\textit{contact law}\ (g^{a}, U^{a}, R^{a})$$

where $\boldsymbol{W}$ is the so-called Delassus operator($\boldsymbol{W} = {}^{T}H\,\boldsymbol{M}^{-1}H$).

The principle of the resolution [10] is summarized in Figures 2 and 3. The contact problem resolution is performed iteratively. An inner loop of iterations (gs_it_1) is performed without checking convergence. Such choice has been done regarding the diffusion of information in the Gauss-Seidel algorithm. An outer loop (gs_it_2) is related to convergence, with respect to the interaction law, for a given tolerance and norm. Those loops can be performed for a fixed number of iterations given by the checking parameter. The total number of iterations performed by the NLGS algorithm can not exceed gs_it_2 x gs_it_1, even if the method has not achieved the convergence.

*Iteration matrix computation (**M**)*
Time loop k
- *Free velocity computation (u_{free})*
- *Contact configuration computation (q_m)*
- *Contact detection*
- ***Contact problem resolution (NLGS algorithm)***
- *Velocity correction ($u_{i+1} = u_{free} + \boldsymbol{M}^{-1} r_{i+1}$)*
- *Update of the kinematics and the configuration*

Halt criteria

Figure 2: Scheme of the algorithm for the resolution of the multi-contact problem (linear case)

Evaluation of all the matrices $\boldsymbol{W}^{\alpha\beta}$
NLGS iterations :
- *Check loop gs_it_2*
  - *Iteration loop gs_it_1*
    - *Contacts α*
      - *Resolution of the local problem*
      - *$U_{i+1}{}^{\alpha} = U_{free}{}^{\alpha} + \sum \boldsymbol{W}^{\alpha\beta} R_{i+1}{}^{\beta}$*
      - *Contact law (g^{a}, U^{a}, R^{a})*
  - *Convergence test (regarding a tolerance and the choice of a norm)*

Figure 3: Scheme of the NLGS algorithm

The presented work aims to better understand the coupling effect of the choice of a physical model together with specific numerical considerations due to the use of a NLGS algorithm in the resolution of the contact problem.

In the present work we focus on the modeling of simple dry masonry structures (columns, basic assembly of panel of bricks) under out-of-plane loading, for a given volumetric model (rigid bodies) and for different writings of the Signorini-Coulomb conditions and for different sets of parameters for the NLGS algorithm. In a first step we give an illustration of the two notions – reliability and quality of the simulation – on the very simple example of a swilling column. The same kind of analysis is then performed on a more realistic structure for which experimental results are available.

3 COLUMN INSTABILITY

The first page must contain the Title, Author(s), Affiliation(s), Keywords, and the Abstract. The second page must begin with the Introduction. The first line of the title is located 3 cm from the top of the printing box.

3.1 Presentation of the study case

A massive column composed of 4 blocks of concrete rosed up without mortar is subjected to rocking phenomena. Each block (1 m x 1m x 1m) is modeled as a rigid body (ρ = 2500 kg/m^3). Interaction law between blocks characterizes frictional contact within a classical Signorini-Coulomb without restitution (Figure 4).

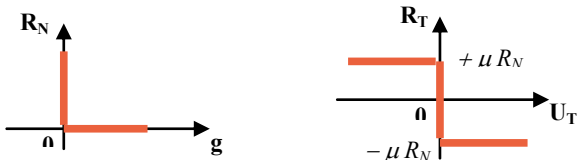

Figure 4: Signorini-Coulomb condition (IQS_CLB law)

The overturning of the column starts after a self-weight period, between t = 0s and t = 0.5s. It is modeled using the rotation (angle α) of the gravity vector $\mathbf{g}^{\alpha}$ up to reach the collapse of the column. Loading phases are summarized in Figure 5.

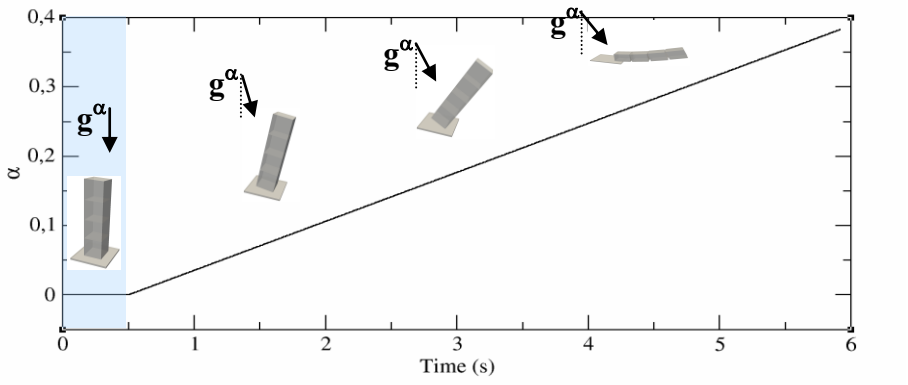

Figure 5: Loading phases modeling the overturning of a simple column – time evolution of α

3.2 Effect of the convergence norm

Whereas all other parameters are kept fixed (number of iterations in the check loop gs_it$_2$, tolerance tol, and choice of the norm) *gs_it$_1$* is first set at 16 iterations, which corresponds to the number of contact points in the column (4 contact surfaces, all discretized with 4 contact points), and then increased by using a multiple of 16 (32 iterations, 48, *etc*). Varying the parameter *gs_it$_1$* is an artificial way to drive the convergence tolerance. Local behaviors – velocities and reactions – are tracked at each contact point.

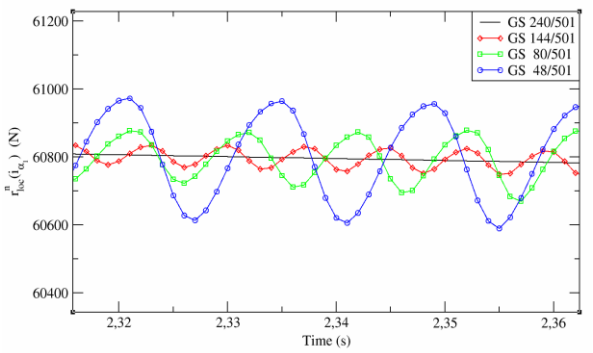

Figure 6: oscillations of the normal local reactions for different configuration of the NLGS algorithm

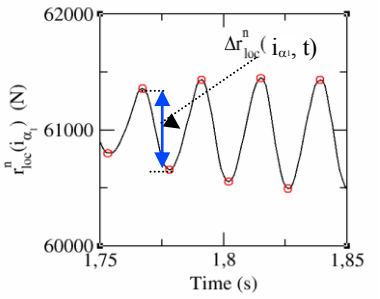

Figure 7: measure of the error due to local oscillations

One of the very first result of this study shows perfectly well the numerical instability affecting the quality of the solution depending on the convergence threshold of the solution. Local reactions (normal or tangential) oscillate around a mean value which appears as the theoretical converged solution expected in the calculation (Figure 6). This imposes to make the distinguish between poor converged solutions and fully converged ones fitting with theoretical solutions. The oscillations of local reactions are purely due to numerical effects. A measure of the error in oscillation of the local reactions may appear as a good criterion of quality for the simulation (Figure 7). The evaluation of the mean amplitude of the oscillations of the local reactions at different contact scale (contact point, surface of contact, *cf.* Figure 8) and generalized to the whole column regarding the number of iterations *gs_it$_1$* performed in the NLGS algorithm (Figure 9) give instructive indications on the behavior of the algorithm.

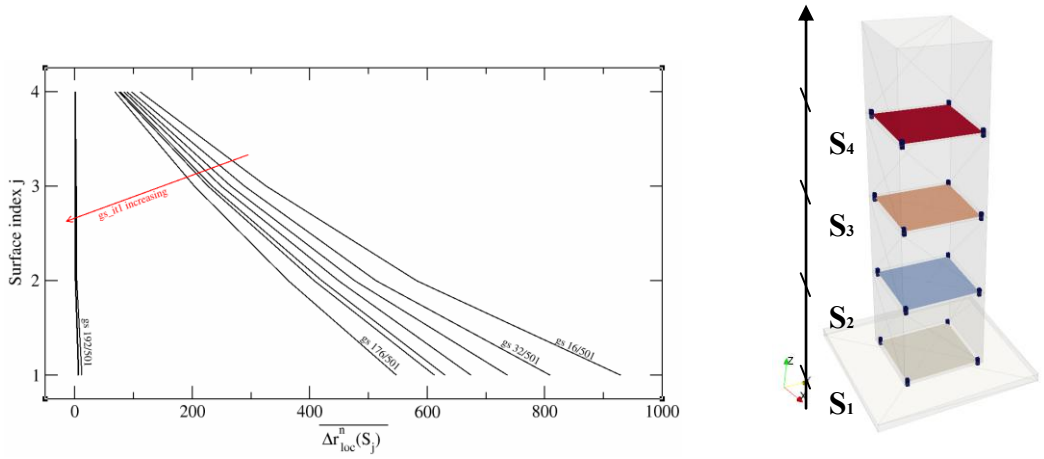

Figure 8: Estimation and repartition of errors due to the oscillations of the normal local reactions for different configuration of the NLGS algorithm at the surface of contact scale

Errors due to the oscillation of local reactions differ in function of their location in the column. Regarding the error – for given gs_it_1 values – at the scale of the surface of contact as the mean value of the error at each contact point belonging to the considered surface, makes possible to identify two phenomena. The upper the surface of contact takes place in the column, the lower is the oscillating error, which can be explained throughout the effects of upper bodies on the considered surface behavior (trimmed oscillations). This can be observed for all gs_it_1 values up to rise a critical value of this parameter from which the error due to the oscillation of the local reactions – normal or tangential – vanishes. The generalization of such a treatment of the estimation of the error at the scale of the whole column using a mean of all the oscillations at the contact points belonging to the column give the same tendency.

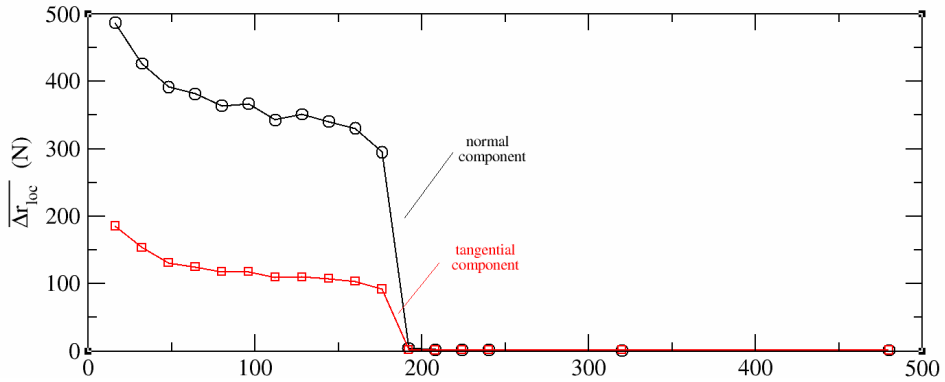

Figure 9: Generalized estimation of the error due to the oscillations of local reactions – for normal and tangential components – at the whole column scale

The same analysis performed on 2 other tested columns with 5 and 6 blocks respectively (Figure 10) shows moreover the dependency of this critical number of NLGS iterations gs_it_1 with the nature of the sample (number of blocks). As explained previously, the variation of the number of iterations gs_it_1 decreases artificially the value of the tolerance for which the test of convergence of the solution is performed. An estimation of the effective tolerance $tol_{effective}$ really driving the convergence of the simulation regarding the chosen one tol_0 is given in Figure 11 depending of gs_it_1 for two different measures of error in the sample from which depend the estimation of the convergence [11]. Error 2 gives an estimation of the variation of velocity in the sample during a Gauss-Seidel iteration, whereas Error 3 give an equivalent estimation for the variation of energy in the sample. Finally convergence occurs if Errors < tol_0.

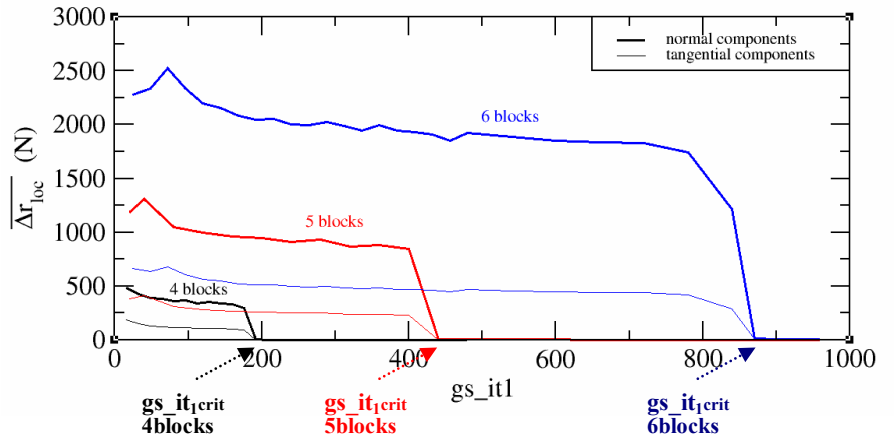

Figure 10: Influence of the number of blocks in the column regarding with the generalized estimation of the error due to the local oscillations

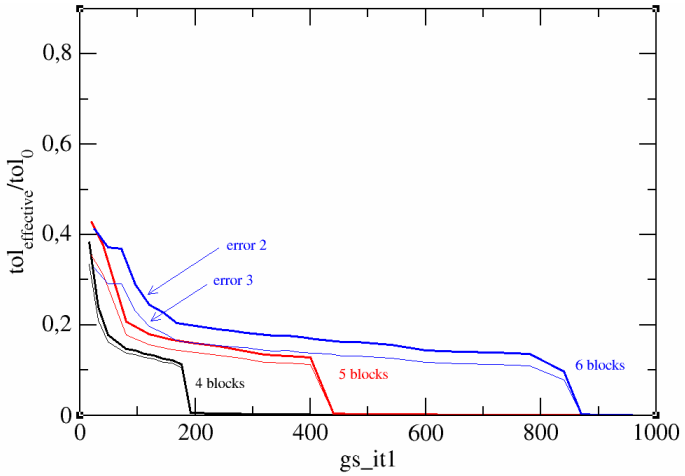

Figure 11: Estimation of the effective tolerance artificially imposed by driving the convergence with GS iterations parameter

3.3 Influence of the model for the Signori-Coulomb condition

Similar tests are performed using a different formalism of the Signorini-Coulomb condition. This model differs from the previous one in the addition of an unilateral elastic behavior in compression for the normal component (Figure 12). The use of such a law might decrease the overestimation of the critical angle due to a full rigid modeling (at the body and at the interface scales). This deformable interaction law acts through a unilateral spring of rigidity $\boldsymbol{k_i}$. The law used previously may appear as a deformable law with an infinite rigidity $\boldsymbol{k_\infty}$. paper.

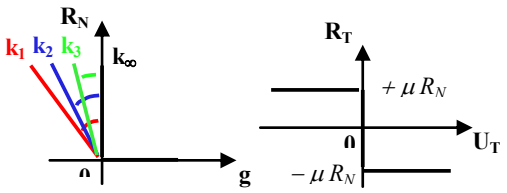

Figure 12: Deformable law (Elastic_Repell_CLB)

Usually the interaction rigidity is set to mimic the deformability of the body. This might give more realistic global behavior of the structure. The rigidity modulus $\boldsymbol{k_i}$ of each spring is consequently defined regarding the influence area of a contact point (here the quarter of the contact surface $S_{1/4}$), the Young modulus of the block E_{brick_i} and its height h_{brick} within the relation $\boldsymbol{k_i} = S_{1/4}$ x E_{brick_i} x h_{brick}. Blocks are characterized by a unique value of the Young's modulus in the whole column. Different cases have been studied so as to evaluate the influence of the stiffness of the blocks and consequently the rigidity of the corresponding springs at the interface. Three of them are presented in this paper, retained values are summarized in Table 1 and are estimated regarding the following reference value $E_{brick\_0} = 1.67\ e^{+10}$ N/m².

Young modulus of blocks	Rigidity modulus at the interace (N/m)
$E_{brick\_1} = 10$ x E_{brick_0}	$k_1 = 4.175\ e^{+10}$
$E_{brick\_2} = 100$ x E_{brick_0}	$k_2 = 4.175\ e^{+11}$
$E_{brick\_3} = 1000$ x E_{brick_0}	$k_3 = 4.175\ e^{+12}$

Table 1: Young's modulus.

The same type of analysis of the results in terms of mean error at the column scale – due to the oscillation of the local reactions at each contact point of the column – are proceeded for those different values of rigidity at the interface (Figure 13). Results are consistent with first observations done for the rigid contact law regarding the existence of a critical gs_it_1. Regarding the error variation toward the elasticity of the interface, the more rigid is the interface between blocks and the closer is the critical number of iteration gs_it_1 of the rigid contact law. In terms of error estimation, the amplitude of the oscillations is much larger when the interface are more rigid to the extent that the oscillation frequency of the spring is increased, which implies that springs are more sensitive to shocks. Results are also given in terms of effective tolerance with respect to the previous analysis (Figure 14).

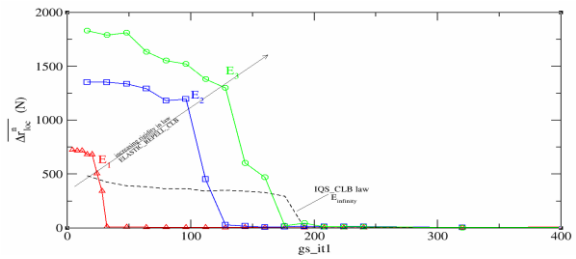

Figure 13: influence of the interface rigidity regarding with the generalized estimation of the error due to the local oscillations for the Elastic_Repell_CLB law

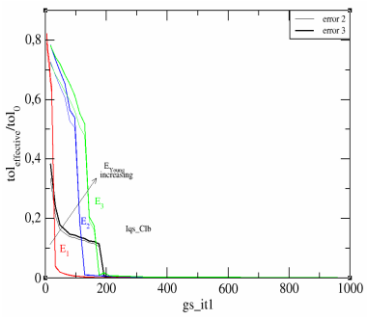

Figure 14: estimation of the effective tolerance artificially imposed for the Elastic_Repell_CLB law

Finally a very last analysis can be performed focusing on the influence on the CPU time. In first approximation, CPU time can basically be estimated throughout the number of iterations of the NLGS algorithm performed during the whole simulation. The results are proposed in Figure 15 by plotting the mean number of GS iterations in terms of the gs_it_1 parameter. This shows once again the existence of critical values of the parameter gs_it_1 for which the mean number of GS iterations performed is equal to the critical value. Depending on their rigidity

springs may trigger the instability of the system and delay the convergence of the algorithm. This phenomenon might be corrected by adding damping in the system.

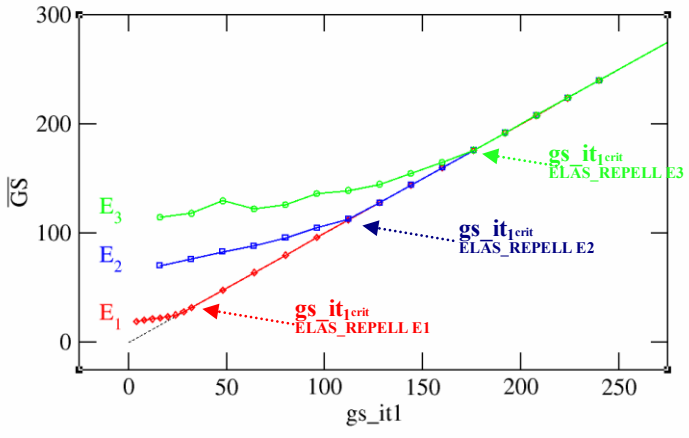

Figure 15: Estimation of the CPU effectiveness basically estimated thanks to the mean number estimation of the GS iterations parameter

3.4 Conclusion

Those simple tests perfectly show the dependency of the quality of the solution regarding with the choice of the NLGS parameters and the effects of the interface law model on the NLGS behavior and on the surrounding effects on the solution. The NLGS parameters are depending on the nature of the problem and the modeling choice. The choice of driving NLGS *gs_it1* parameter for a fixed tolerance seem not to be well adapted. No trivial relationships have been identified regarding the existence of the critical value of this parameter and the nature of the studied case. Only dependency has been highlighted. The next part of this work aims to proceed to the study of the numerical behavior of a more complex structure for which experimental tests have been performed. The purpose is to estimate the impact NLGS parameter on the global physical behavior of a real structure.

.

4 INFLUENCE OF THE NUMERICAL INSTABILITY ON A REALISTIC STRUCTURE – GLOBAL BEHAVIOR

4.1 Presentation of the study case

A series of static tests have been performed in the Laboratory of the Department of Structural Mechanics of the University of Pavia in Italy [13]. Those tests consist in the study of dry masonry structures submitted to out-of-plane loading. Masonry specimens 1:5 scale were tested on an inclined plane machine so as to determine experimentally the activation multiplier α defined as the ratio of horizontal and gravitational accelerations, and which appears as the critical instability angle for which the masonry specimen only subjected to self-weight placed on the table becomes unstable. The activation multiplier α was measured by means of a plumb line placed at one side of the machine and converting the obtained quantity into an

inclination angle. According to the work of D'Ayala and Speranza [14] on the definition of mechanisms of collapse of historic masonry buildings, a total of 42 stone masonry specimens representative of several configurations of out-of-plane collapse mechanisms were tested. The following study focuses on the configuration S24 according with the reported tests classification (Figure 16). This specimen is an assembly of two side walls and a front wall with two window openings with wood lintel beam. As the other ones, the specimen was built with dry stone masonry blocks of marble. The choice of this material amongst shale and granitic stones have been done due to the accuracy on the cutting, the durability of the material and an appropriate friction coefficient. Specimens are typically built with 28 x 80 x 40 mm blocks. The friction coefficient μ in the joint was estimated thanks to measures for three different values of normal stress, using a couple of blocks on an inclined plane ($0.67 \leq \mu \leq 0.77$).

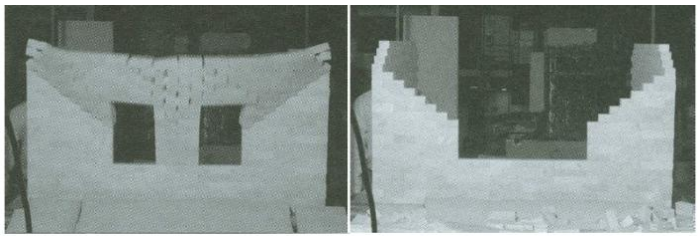

Figure 16: Masonry specimen S24 collapsing (University of Pavia, Italy)

4.2 Modeling options and estimation of the instability of the structure

Modeling strategy used previously in the simple study case is kept. Masonry blocks are modeled as rigid bodies (ρ = 2732 kg/m^3) and behavior between blocks is modeled thanks to the same interface laws characterizing friction. Static coefficient of friction used in the following computations is taken equal to 0.67. The use of such constant value in the whole structure is discussed in Section 3.4. More generally it tackles the issue of the initial state of the specimen. Concerning the loading of the sample, three phases have been identified (Figure 17). The masonry is first of all kept under self-weight, then inclination occurs to reach an inclined state of the table. The very last phases of the loading consists in keeping the specimen under self-weight in the tested inclined state so as to check its stability (relaxation). The inclination of the table has been taken into account throughout the rotation of the gravity with a constant rotation velocity $d\alpha/dt$. The duration of the loading phase consisting in

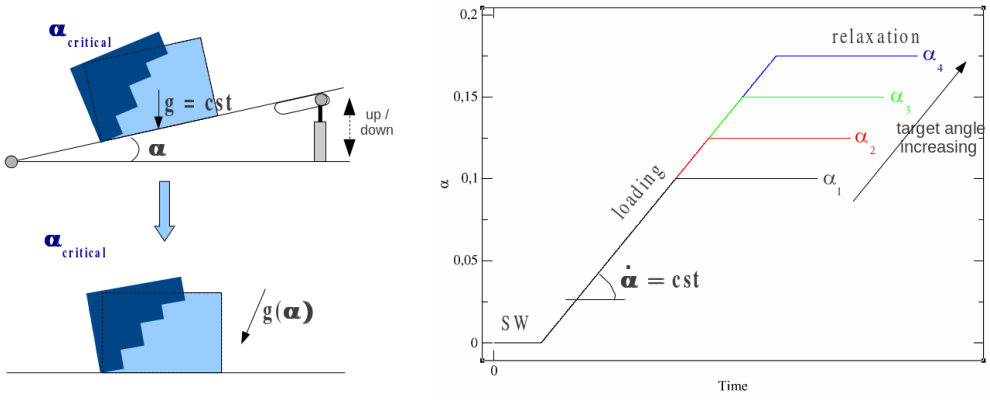

Figure 17: Loading phases

inclining the table has been carefully managed so as to guarantee the non existence of inertia phenomena. Tests of dependency regarding the rotation velocity have also been performed but are not presented in this paper. The test aims to determine instability angle for which the structure collapse. A series of numerical simulation are performed to define this value. The stability is checked throughout kinetic energy considerations (Figure 18). The kinetic energy of the specimen is tracked during the simulation. It allows both to control the non existence of inertia phenomena and to deal with the stability state of the structure.

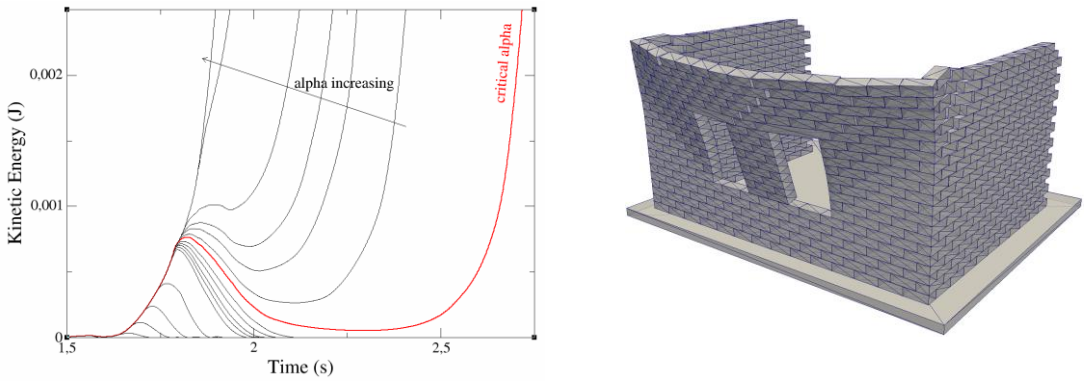

Figure 18: Estimation of the overturning of the specimen thanks to kinematic considerations and visualization with ParaView of a result of simulation obtained with LMGC90

4.3 Tested parameters at the origin of the numerical instability of the structure

As illustrated with the simple example of the column submitted to overturning phenomena, the choice of modeling strategy and numerical parameters may be at the origin of numerical instability. This instability depends also on the sample. The purpose of this part is to measure the influence of this numerical instability on the whole physical behavior of the structure characterized by the instability angle α. The behavior of masonry specimens are studied regarding different parameters of NLGS (number of iterations, tolerance, contact ordering, etc) and different modeling of the Signorini-Coulomb condition. A new model taken into account viscous damping and elasticity is used in complement of the two previous ones.

4.4 Full rigid model

Simulations are first of all performed with a classical modeling of friction (no regularization and no viscous damping). Effects of the variation of the NLGS parameters on the behavior of the specimen are studied. Within the same type of scheme, variations on iterative loops of the NLGS algorithm are performed. The tolerance used to check the convergence of the algorithm is artificially decreased by increasing the number of iterations to perform before each test of convergence (variation of the gs_it_1 parameter). The evolution of the critical instability angle obtained is drawn in Figure 19. The results are consistent with those established with the simple column tests. It shows the existence of a critical value of the parameter gs_it_1 from which it is possible to distinguish poorly converged solution and totally converged one. The error ε_{cv}, defined as the ratio $\Delta_{cv} / \alpha_{crit,\,cv}$ where $\alpha_{crit,\,cv}$ the fully converged angle and Δ_{cv} is the difference between poorly converged instability angle and fully converged one ($\Delta_{cv} = \max\{ \mid \alpha_{crit,\,cv} - \alpha_{crit,\,gs\_it1} \mid, gs\_it_1 \}$), may be considered as a first measure of the convergence error. Regarding this first set of NLGS parameters (fixed choice of the tolerance and norm, fixed reading of the contact data set), this error is estimated at $\varepsilon_{cv} = 5.17$ %.

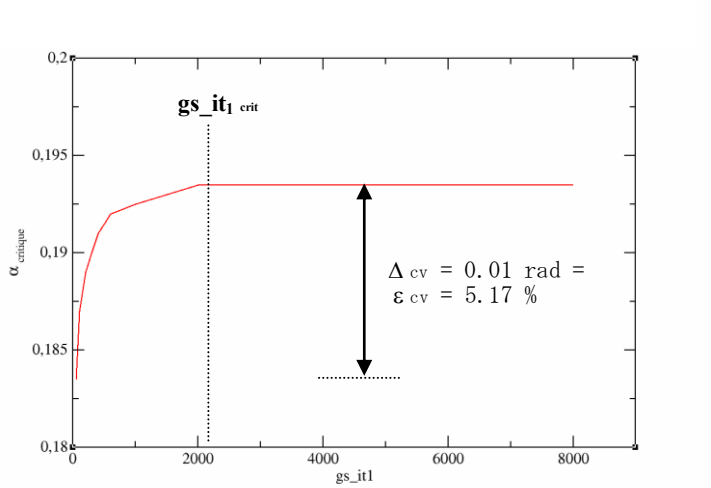

Figure 19: Estimation of the error on the converged critical instability angle

A second series of simulations is performed to illustrate the behavior of the NLGS algorithm, focusing on the convergence tolerance (Figure 20). Tests are proceeded for several configurations of the NLGS parameters leading to different level of quality of the converged solution. Tolerance parameter value can be decreased so as to minimize local errors at contact points as illustrated with the column test. Independently on other NLGS parameters used, the fully converged solution is reached for enough severe tolerance. Here the effect of tolerance decreasing is artificially obtained decreasing *gs_it1* parameter.

A very last series of simulations is performed to test the influence of the contact ordering on the behavior of the structure (Figure 21). This point has not really been highlighted in the basic presentation of the NLGS algorithm. Since the frictional contact problem admits several solutions the way contact are ordered has an impact on the selected solution. However the variability $\varepsilon_{cv}^{ctc\ set}$ observed between converged solutions can be estimated on this example around 1.3 %.

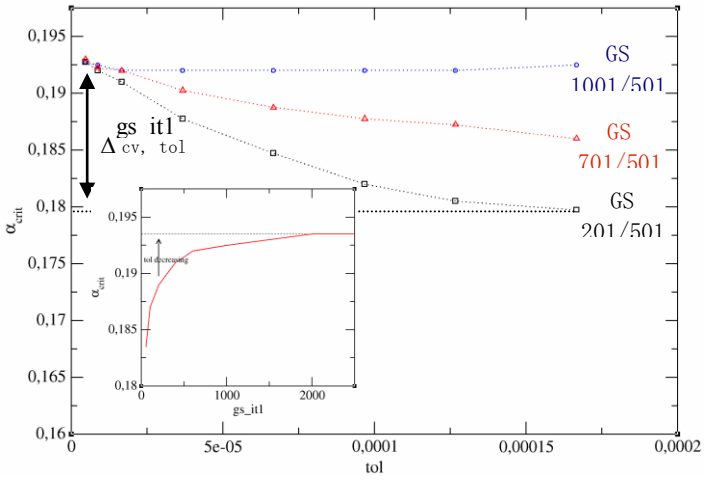

Figure 20: Influence of the tolerance on the convergence
for different configurations of the GS algorithm

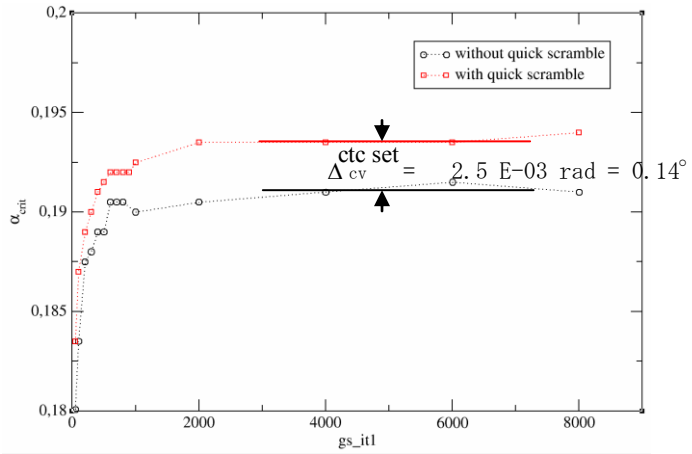

Figure 21: Difference on the fully converged instability angle due to the reading contact data set

Reliability of numerical results can also be considered comparing them with the experimental instability angles measured during the test. The fluctuation ε_{num} between experimental and numerical results is defined as the ratio Δ_{num} / $\alpha_{crit,\ exp}$ where $\alpha_{crit,\ exp}$ is the experimental value of the instability angle ($\alpha_{crit,\ exp}$ = 0.156) and the Δ_{num} difference between the experimental and numerical angles ($\Delta_{num} = | \alpha_{crit,\ cv} - \alpha_{crit,\ exp} |$). With rigid blocks and inelastic interface model, this fluctuation is quiet important ($\varepsilon_{num}^{rigid}$ = 24%). It should be explained throughout the over estimation of the mechanical stiffness due to the use of a full rigid model. Effect of elasticity in the interface model is discussed in Section 3.6.

4.5 Rigid bulk behavior with randomly assigned friction coefficient interface

The influence of the coefficient of friction on the stability of the structure is trivially and basically shown in Figure 22. For uniform distributions, the smaller is the friction coefficient and the sooner the instability angle is reached. Regarding with the important variation of the coefficient of friction found experimentally ($0.67 \leq \mu \leq 0.77$) to characterize friction between blocks, we can reasonably assume a non uniform distribution of the friction coefficient in the whole structure.

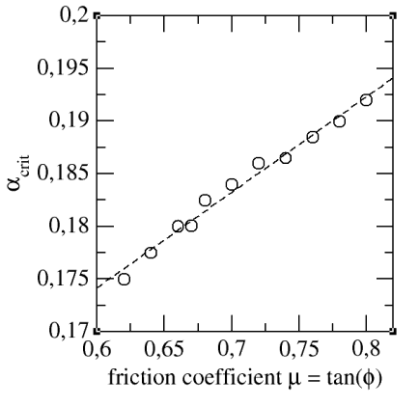

Figure 22: Evolution of the critical instability angle in function of the coefficient of friction uniformly set on the structure

A series of simulations is performed to discuss the influence of the initial state of the structure and to deal with more realistic study case of non ideal structures. Variability of the coefficient of friction is taken into account in the model. Values of the coefficient of friction are randomly assigned within a normal distribution (π, σ) at each contact point (Figure 23). This aims to model asperity of blocks through out a non uniform interface behavior. The difference between the probability density function corresponding to the distribution of the coefficients of friction in a given sample and the target one can be explained regarding with the small number of draws performed to realize the statistic. This implies in our case the restriction of the variation of the coefficients of friction around the mean value $\pi = 0.67$.

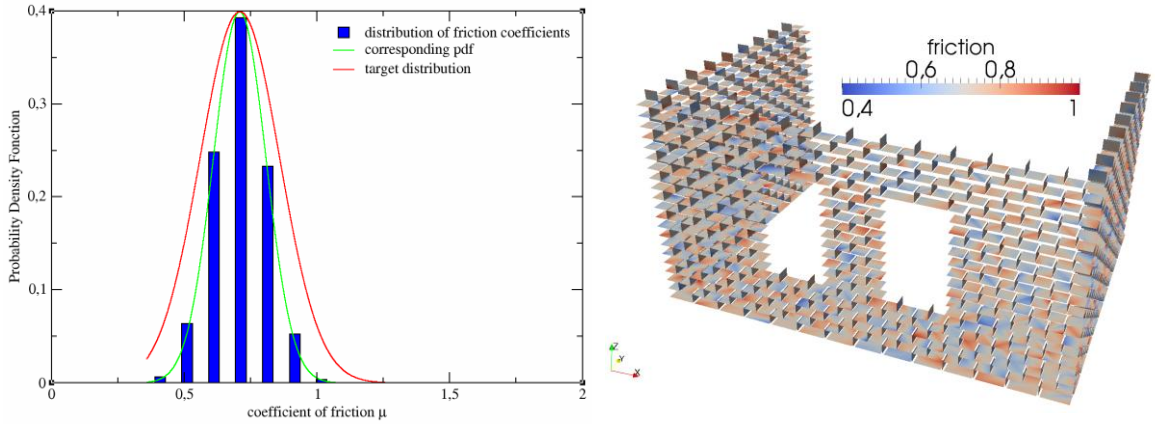

Figure 23: Randomly assigned friction within a normal distribution (π, σ)

Nearly 200 draws are performed for 4 different values of the gs_it_1 parameter ($gs\_it_1 = 51$, 201, 501 and 1001) whereas other parameters are kept fixed (gs_it_2 and tol). Critical values of the angle of instability for the different draws are given in Figure 24. Results are compared with the ones obtained with uniform coefficient of friction (Figure 25).

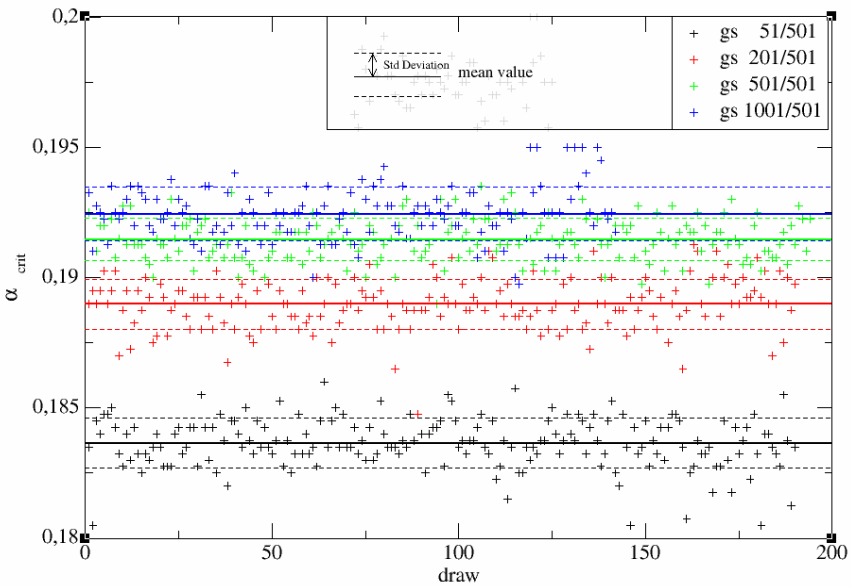

Figure 24: Instability angles for different configurations of the initial state of the structure (randomly assigned friction coefficients) and for different values of the gs_it_1 parameter

Considering randomly assigned friction, it appears clearly that the introduction of such a variability on this parameter may impact the collapse of the structure making the structure more or less prone to overturning phenomena. It has to be noticed that the mean values of critical angles obtained stay very closed from the one corresponding to the full rigid model with a uniform friction. Eventually, the variability on the coefficient of friction give an estimation of the error introduced when using ideal structures.

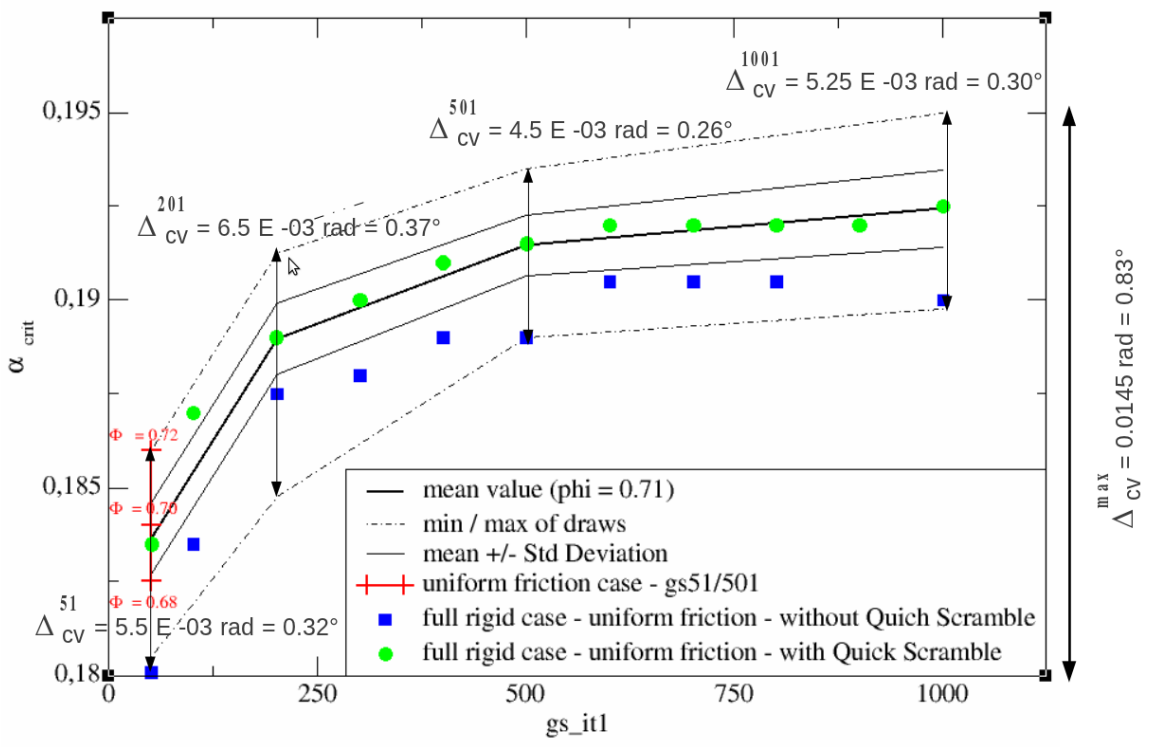

Figure 25: Comparison of critical angles found for uniform or randomly assigned coefficients of friction

4.6 Rigid bulk behavior with elastic interface

Simulations are performed using five values of stiffness around a given reference value, which is obtained such as the relative displacement of objects due to compression is equivalent to the one obtained with deformable objects with a given Young's modulus (E_0 = 2.6 e^{+10} N/m² standing for a marble). Those values are reported in Table 2. It covers, once again, a large range of values illustrating the influence of this formalism on the description of the contact behavior (Figure 21). Regarding the efficiency of the convergence, it clearly appears that the smoother the rigidity of the spring is, the faster the convergence appears. However the system is disturbed by local oscillations due to the springs which takes time to be damped (numerically or physically).

Young Modulus of blocks	$E_2 = E_0/10$	$E_4 = (E_1+E_2)/2$	$E_1 = E_0$	$E_5 = (E_1+E_3)/2$	$E_3 = E_0$ x 10
Rigidity modulus at the interface (MN/m)	k_2 = 74	k_4 = 409	k_1 = 743	k_5 = 4085	k_3 = 7429

Table 2: Tested Young's modulus and equivalent interface rigidity.

4.7 Damping effect on elastic interfaces

Simulations have been performed by adding viscous damping in the Signorini-Coulomb model [9]. This method makes possible to take benefit of the elasticity without wasting time due to springs oscillations. This pure phenomenological law, introducing elasticity and viscosity parameters, aims to introduce interface deformation damping oscillations at the structure level.

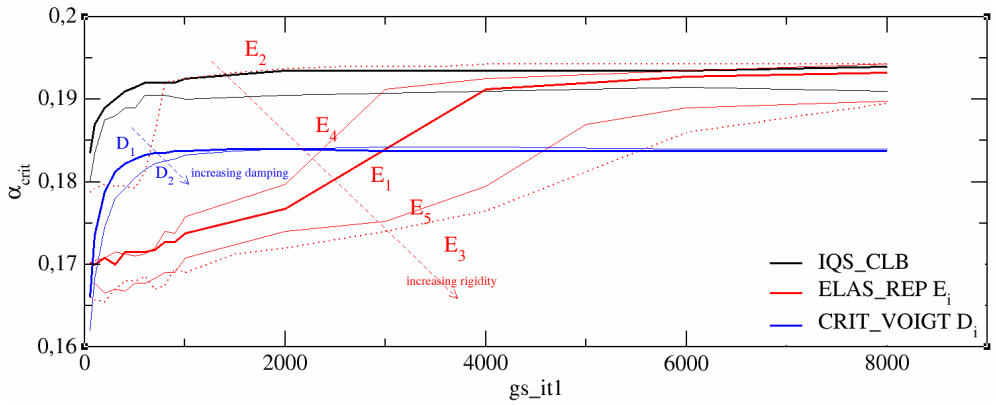

Figure 26: Estimation of the errors on the converged
critical instability angle values for the different tested laws

Results presented in Figure 26 are once again consistent with previous analysis performed in this work. Effect of convergence norm can be easily identified. The dependency of the solutions with regard to the variation of critical viscous damping has not been really highlighted. Only two different values of the damping parameter ($\boldsymbol{D_i}$) have been tested. The difference obtained for collapsing angle can be explained by the fact that the viscous model also modify the tangential behavior.

Figure 27 presents the whole results of this work throughout tolerance considerations. As previously explained with the simple study case of the column, an effective tolerance value can be estimated from results obtained using variation on GS parameters. This representation of the results points out the efficiency of this contact law regarding the other ones.

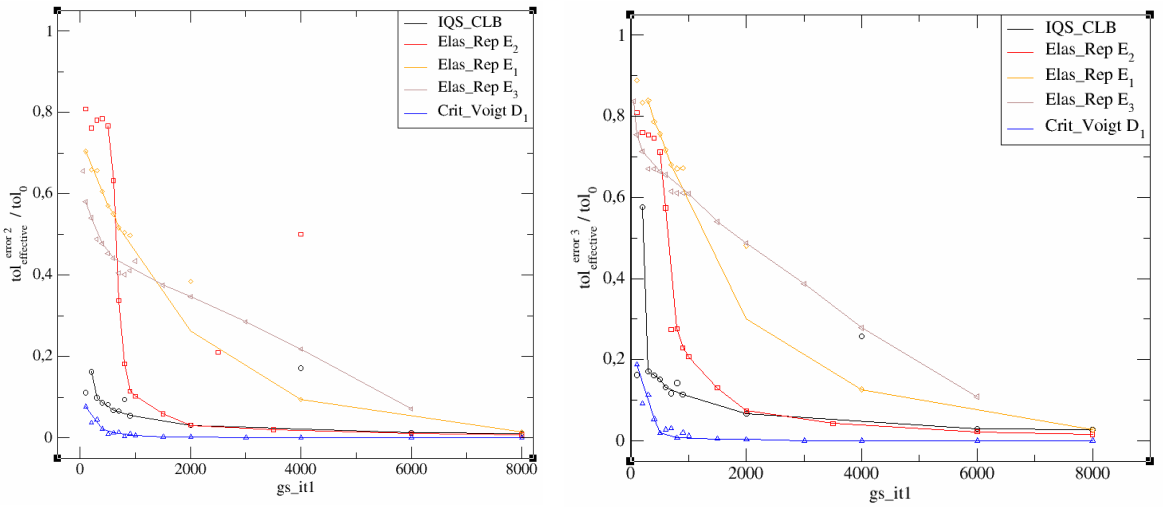

Figure 27: Estimation of the effective tolerance artificially imposed for the three tested laws regarding two types of error (error 2 and error 3 defined in 2.2)

.

4.8 Conclusion

This study has showed the influence of the choice of the NLGS parameters. The choice of the frictional contact model has an influence on the NLGS method. Nonetheless, it clearly appears that the choice of a different model gives similar global behavior, but may have significant impact on the duration of the calculation. Finally, it also has to be noticed that numerical instability coming from a poor convergence can have a real influence on the global behavior of the structure.

5 CONCLUSION AND PERSPECTIVES

As it can be explicitly noticed regarding the theoretical expression of the problem to be solved using the NSCD method, and regarding the choice of the use of the NLGS algorithm to solve it, it clearly appears that the choice of modeling options – throughout the definition of volumetric and interface models whose depends the physical reliability of the whole simulation – and the definition of a configuration of the NLGS algorithm insuring to sort out the problem within a given level of quality, are deeply related. This works shows the dependency of the choice of the parameters of the NLGS algorithm on the local and global behaviors of the sample, and points out the influence of the choice of the formalism of the interface model on the algorithm behavior. Eventually the level of the quality of the simulation have been discussed regarding those factors. However the reliability of simulation governing by the choice of both the volumetric model and the interface one has not been enough studied. The variation of the interface model used to deal with the study of the reliability of the model are being completed with other tests involving the deformability of blocks belonging to the masonry and the influence of their space-discretization.

REFERENCES

[1] P.A. Cundall. A computer model for simulating progressive large scale movements of blocky rock systems. *In Symposium of the International Society of Rock Mechanics*, volume 1, pages 132-150, 1971.

[2] P.A. Cundall and O.D.L. Strack. A discrete numerical model for granular assemblies. Geotechnics, 29 (1): 47-65, 1979.M. Jean, J.J. Moreau. Unilaterality and dry friction in the dynamic of rigid body collections, *Proc. Contact Mechanics Int. Symp.*, Edt A. Curnier, 31-48, 1992.

[3] M. Jean and J.J. Moreau. Unilaterality and dry friction in the dynamic of rigid body collections. *Proc. Contact Mechanics Int. Symp.*, Edt A. Curnier, pages 31-48, 1992.

[4] J.J. Moreau. Unilateral contact and dry friction in finited freedom dynamics. *CISM Races and Readings*, 302 Springer-Verlag, pages 1-82, 1988.

[5] M. Jean. Frictional contact in collections of rigid and deformable bodies: numerical simulation of geomaterials. Mechanics of geomaterials Interfaces, *A.P.S. Saladurai and Mr. JJ. Bolt*, eds., Elsevier Science, Amsterdam, pages 463-486, 1995.

[6] M. Jean. The non-smooth contact dynamic method computer methods in applied mechanics and engineering. *Comput. Methods appl. mech. Eng.*, 177, No 3-4, 235-257, 1999.

[7] F. Dubois, M. Jean. Une plateforme de développement dédiée à la modélisation des problèmes d'intéraction, *In M. Pottier-Ferry, M. Bonnet et A. Bignonnet*, éditeurs: 6ème Colloque National en Calcul des Structures, Giens, volume 1, 111-118, 2003.

[8] F. Dubois, M. Jean, M. Renouf, R. Mozul, A. Martin, M. Bagnéris. LMGC90, 11ème Colloque National en Calcul des Structures, Giens, 2011.

[9] F. Radjaï et F. Dubois. Discrete-Element Modeling of Granular Materials, *ISTE Ltd and John Wiley & Sons Inc*, 2011.

[10] F. Dubois and M. Renouf. Discrete Element Methods for the simulation of divided media, LMGC90's manuals (https://subver.lmgc.univ-montp2.fr/LMGC90v2), 2008.

[11] B. Cambou, M. Jean and F. Radjai, Michromechanics of Granular Material, *Wiley-ISTE*, 2009.

[12] M. Jean, Quelques manières de traiter le contact unilatéral et le frottement sec, documentation du logiciel LMGC90, 2005.

[13] L. F. Restrepo-Vélez, G. Magenes. Static Tests on Dry Stone Masonry and Evaluation of Static Collapse Multipliers. *Research Report ROSE 2010/02*, Iuss Press, Pavia, Italy, 2010.

[14] D. D'Ayala, E. Speranza. Definition of collapse mechanisms and seismic vulnerability of masonry structures. *Earthquake Spectra*, Volume 19, Issue 3, 479-509, 2003.